Journal of Applied Electrochemistry (2005) 35:459–465
DOI 10.1007/s10800-004-8346-2

Electrochemical synthesis of perovskite oxides

G. HELEN ANNAL THERESE, M. DINAMANI and P. VISHNU KAMATH*
Department of Chemistry, Central College, Bangalore University, Bangalore, 560 001, India
*(*author for correspondence: e-mail: vishnukamath8@hotmail.com)*

Received 9 July 2004; accepted in revised form 12 December 2004

Key words: electrosynthesis, cathodic reduction, perovskite oxides

Abstract

Hydroxide precursors to perovskite oxides of the formula, $LnMO_3$ (Ln = La, Pr, Nd; M = Al, Mn, Fe) and $LaMO_3$ (M = Co and Ni) were synthesized by electrogeneration of base by cathodic reduction of the appropriate mixed-metal nitrate solution. The precursors were heat treated at different temperatures to obtain the perovskite oxides. The bath composition for various systems was optimized to get a single-phase oxide product. This method can be adapted as a simple route to the synthesis of perovskite oxide coatings on conducting substrates.

1. Introduction

Perovskite oxides are an important class of compounds in solid state and materials chemistry. Perovskites of the general formula, $LnMO_3$ [Ln = Rare earth metal ion; M = transition metal ion/Al^{3+}] have a wide range of electrical and magnetic properties [1]. $LaNiO_3$ is metallic on account of the strong O–M–O interactions [2] while $LaCoO_3$ is a room temperature insulator and undergoes an insulator $\rightarrow$ metal transition at 1200 K [3]. $LaCoO_3$ has been successfully used as redox catalyst for NO and CO gases in automobile exhausts [4]. $LaMnO_3$ exhibits colossal magnetoresistance [5] and also finds application as an electrode in solid oxide fuel cells [6]. $LaAlO_3$ is used as a substrate for the deposition of oriented oxide films for device based applications [7]. $LaFeO_3$ also finds application as an electrode material for catalysis of oxygen evolution [8].

For the successful use of these materials in working devices, it is commonly necessary to obtain them in the form of thin films deposited singly or in a layer-by-layer configuration. Conventionally films of perovskite oxides are synthesized by pulsed laser deposition (PLD) [9], rf sputtering [10], electron/ion beam etching or MOCVD [11]. However, these routes are capital and energy intensive and require an ultrahigh vacuum system in addition to a high-power laser/ion source. Electrochemical synthesis [12, 13], on the other hand, offers a simple and inexpensive route to the preparation of hydroxide/oxide coatings.

Matsumoto and coworkers [14–17] have made significant contributions towards the anodic electrosynthesis of perovskite oxides $LnMO_3$(M = Mn, Co). Their studies have shown that even though Ln^{3+} ions do not participate in any oxidation reactions, they can be incorporated into the anodically grown oxide-hydroxide films of Mn and Co provided a very high Ln^{3+}/M ratio (10^2–10^3) is maintained in the bath. These syntheses were carried out potentiostatically in mixed-metal ($Ln^{3+} + M^{2+}$) nitrate/acetate baths at potentials appropriate to deposit the $M_2O_3 \cdot H_2O$ [2MO(OH)] film. The Ln^{3+} ions were incorporated in these films by adsorption to yield a composite film of the composition [$M_2O_3 \cdot 2Ln(NO_3)_3 \cdot yH_2O$]. Thermal decomposition (500–1000 °C) of the composite film was found to yield the perovskite oxide $LnMO_3$. A similar approach for the $La^{3+} + Ni^{2+}$ system resulted in the formation of $La_4Ni_3O_{10}$ [18].

The greatest disadvantage of this technique is that Ln^{3+} ions have no anodic reactions of their own; Ln^{3+} incorporation in the anodic deposit is achieved by enriching the bath with Ln^{3+} ions and its consequent adsorption. This gives poor control over the Ln^{3+} content in the coating. To overcome this difficulty, we employed the electrogeneration of base by the cathodic reduction of a mixed-metal ($Ln^{3+} + M^{2+}/M^{3+}$) nitrate bath. Nitrate reduction results in a steep increase in the pH of the bath close to the electrode and results in the codeposition of both the Ln^{3+} and M^{2+}/M^{3+} ions as their respective hydroxides. Using this method, coatings of $LaMnO_3$ were fabricated [19]. In this paper we extend the cathodic reduction strategy to the synthesis of the family of perovskite oxides $LnMO_3$ [Ln = La, Pr, Nd; M = Al, Mn, Fe]. $LaNiO_3$ and $LaCoO_3$ have also been obtained as single-phase polycrystalline powders. In an illustrative case, that of $LaAlO_3$, adherent films were obtained on stainless steel substrates.

2. Experimental details

The hydroxide precursors were obtained by cathodic reduction of a mixed-metal nitrate solution (total concentration 0.15–0.2 M) containing both Ln^{3+} and M^{2+} (M^{3+} in the case Al and Fe) ions. The experimental conditions were different for different systems and are listed in Table 1. Stainless steel flags (surface area, 2 to 8 cm^2) were used as cathodes for the preparation of coatings. A cylindrical Pt-mesh (geometric area, 28 cm^2) was used as a counter. A uniform coating of the precursor to $LaAlO_3$ could be obtained in 2 h at a current density of 10 mA cm^{-2}. After deposition, the coating was rinsed with water and dried at 80–100 °C. To obtain the oxide, the hydroxide coated flag was inserted into a preheated furnace at 950 °C for 2 h. Thick coatings could be obtained by repeated deposition and thermal treatment of the coating. Gram quantities of the precursor material could be obtained by prolonged deposition (4–5 h) at higher current densities (25–50 mA cm^{-2}) in a divided cell using Pt flags as working and counter electrodes. A KNO_3 solution having the same concentration as the mixed-metal nitrate bath was taken in the anode chamber. During electrolysis, the product formed thickens and detaches itself from the electrode and settles at the bottom of the cathode chamber. Despite the possibility of re-dissolution, the hydroxide precursors could be recovered as the rare-earth hydroxides have low solubility products. The products recovered by filtration were washed free of anions and dried at 80–100 °C to constant weight. These precursors were subjected to thermogravimetric analysis (lab. built system, heating rate 5 °C min^{-1}) to determine their decomposition temperature. They were then decomposed at the required temperatures to obtain the corresponding oxides (see Table 2).

While Mn^{2+} and Co^{2+} in their respective hydroxide precursors are oxidized to their trivalent states during work up of the coating and thermal treatment [19, 20], in the La–Ni system, the oxidation of Ni^{2+} to Ni^{3+} has been achieved electrochemically by polarizing the La, Ni-hydroxide coating anodically in 6 M KOH at a very low current density of 1 mA cm^{-2} for 15 min to oxidize the Ni^{2+} to Ni^{3+}. Since La^{3+} has no electrochemical reaction, only Ni^{2+} gets oxidized anodically by the following reaction well known to alkaline battery chemists [21, 22]

$$Ni(OH)_2 + OH^- \rightarrow NiO(OH) + H_2O + 1e^-$$

The coating blackened upon oxidation and the oxidized coating was scraped off and collected in the crucible for further processing. The procedure was repeated three times to collect a sufficient amount of material. Thermal decomposition of the La–Ni hydroxide was carried out at 550 °C (1 h) in a preheated furnace.

In all the experiments, the working electrode was cleaned with detergent and electrochemically polished prior to electrodeposition as described elsewhere [23].

All electrosynthesized samples were analyzed by powder X-ray diffraction (JEOL Model JDX8P powder diffractometer, Cu Kα source, λ = 1.541 Å) and IR spectroscopy (Nicolet model Impact 400D FTIR spectrometer, KBr pellets, 4 cm^{-1} resolution).

Table 2. TG data of the mixed hydroxide precursors to perovskite oxides

Compound	% Weight loss		T/°C
	Expected	Observed	
$LaAlO_3$	20.17	30.1	950
$PrAlO_3$	20.00	28.6	950
$NdAlO_3$	19.78	29.1	950
$LaFeO_3$	18.21	20.2	950
$PrFeO_3$	18.09	19.2	950
$NdFeO_3$	17.89	20.3	950
$PrMnO_3$	12.97	12.13	675
$NdMnO_3$	12.81	13.41	675
$LaCoO_3$	27.0	27.5	950
$LaNiO_3$	–	–	550

3. Results and discussion

Cathodic reduction of aqueous metal nitrate solutions results in a steep increase in the pH close to the electrode. A number of reactions are responsible for

Table 1. The experimental conditions used for synthesis and the cell parameters of the perovskites obtained after heat treatment

Compound	Electrolyte used			Crystal system JCPDS-PDF	Cell parameters/Å		
	Ln/M	Conc./M	pH		*a*	*b*	*c*
$LaAlO_3$	0.42	0.15	2.58	Rhombohedral 31–22	5.36	–	13.11
$PrAlO_3$	0.33	0.15	3.15	Rhombohedral 29–76	5.33	–	12.97
$NdAlO_3$	0.33	0.15	2.15	Rhombohedral 39–487	5.32	–	12.91
$LaFeO_3$	0.66	0.15	1.95	Orthorhombic 37–1493	5.57	7.86	5.55
$PrFeO_3$	0.66	0.15	0.90	Orthorhombic 15–134	5.48	5.58	7.79
$NdFeO_3$	0.66	0.15	1.89	Orthorhombic 25–1149	5.58	7.76	5.45
$PrMnO_3$	0.66	0.15	1.10	Pseudocubic	3.87	–	–
$NdMnO_3$	0.66	0.15	2.23	Pseudocubic	3.86	–	–
$LaCoO_3$	0.66	0.2	2.68	Rhombohedral 25–1060	5.44	–	13.08
$LaNiO_3$	0.66	0.2	2.45	Rhombohedral 34–1181	5.45	–	6.56

electrogeneration of base [24]. Of these, the most significant ones are the nitrate reduction reactions [25].

$$NO_3^- + H_2O + 2e^- \rightarrow NO_2^- + 2OH^- \quad E^0 = 0.01\ V$$

$$NO_3^- + 7H_2O + 8e^- \rightarrow NH_4^+ + 10OH^-$$

This leads to the electrodeposition of the metal hydroxide on the cathode as

$$M^{n+} + nOH^- \rightarrow M(OH)_n \downarrow .$$

Thus, electroreduction of $Ln(NO_3)_3$ (Ln = La, Pr, Nd) solutions yields the corresponding hydroxide $Ln(OH)_3$ [26]. Electroreduction of M^{3+}/M^{2+} nitrates ($M^{3+} = Al^{3+}$, Fe^{3+}; $M^{2+} = Mn^{2+}$, Co^{2+}, Ni^{2+}) yields the respective oxide gels/hydroxides [27]. When a mixed-metal ($Ln^{3+} + M^{2+}/M^{3+}$) nitrate solution is reduced, the resultant product is not simply a mixture of the two hydroxides, but is X-ray amorphous, showing that there is an intimate interaction between the two phases. We therefore attempted to characterize the hydroxide precursors by IR spectroscopy. In Figure 1, we show an illustrative IR spectrum of a mixed-metal hydroxide and compare it with the spectra of the constituent unitary hydroxides. $Nd(OH)_3$ shows a sharp OH stretching frequency (3650 cm^{-1}) and a strong absorption corresponding to the fingerprint of loosely bound nitrates (1385 cm^{-1}). $Al(OH)_3$, on the other hand, shows a sharp absorption at 1050 cm^{-1} due to the Al–O stretching vibration. The mixed hydroxide precursor shows features due to both the hydroxide constituents.

The mass losses exhibited by the hydroxide precursors on thermogravimetric analyses are listed in Table 2. The observed mass losses could be fitted to the following decomposition reactions:

$$Ln(OH)_3 \cdot MnO(OH) \rightarrow LnMnO_3 + 2H_2O \qquad (1)$$

$$La(OH)_3 \cdot Co(OH)_2 \cdot 3H_2O \rightarrow LaCoO_3 + 5H_2O \qquad (2)$$

$$LnM(OH)_6 \rightarrow LnMO_3 + 3H_2O \qquad (3)$$

Reaction (3) is valid for the M^{3+} = Fe system. The other precursors could not be fitted to any of these possibilities probably due to the presence of anions in the mixed hydroxide.

Further evidence for the decomposition of the hydroxide precursors is seen in the IR spectra. In Figure 2, an illustrative IR spectrum of the La–Co system before and after thermal decomposition is shown. The disappearance of strong absorption corresponding to OH and NO_3^- groups of the mixed hydroxide shows the formation of an oxide residue upon heat treatment.

The XRD patterns of the products of decomposition are given in Figures 3–7. The observed Bragg reflections

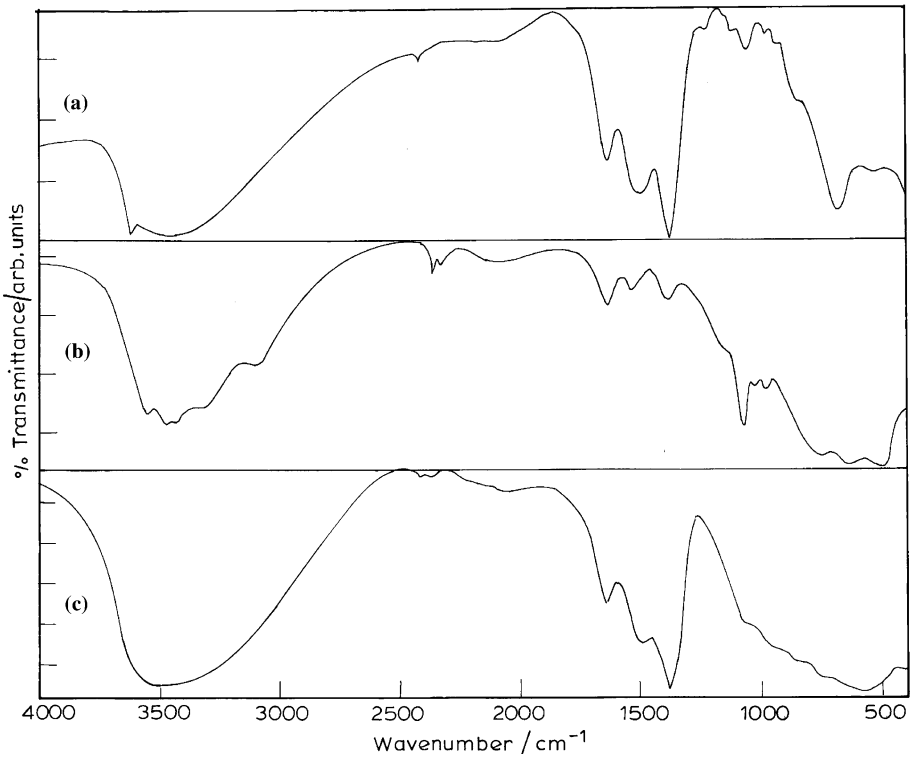

Fig. 1. Infrared spectra of (a) Nd–Al hydroxide precursor compared with the spectra of (b) $Al(OH)_3$ and (c) $Nd(OH)_3$.

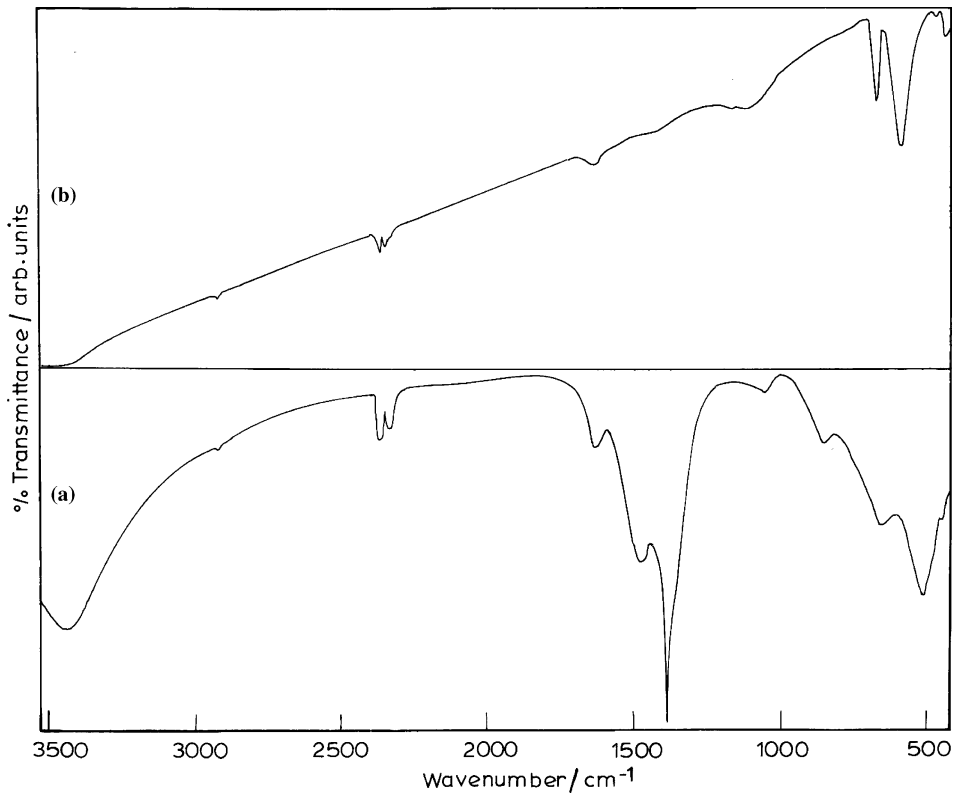

Fig. 2. Infrared spectra of the LaCo-hydroxide (a) before and (b) after heat treatment.

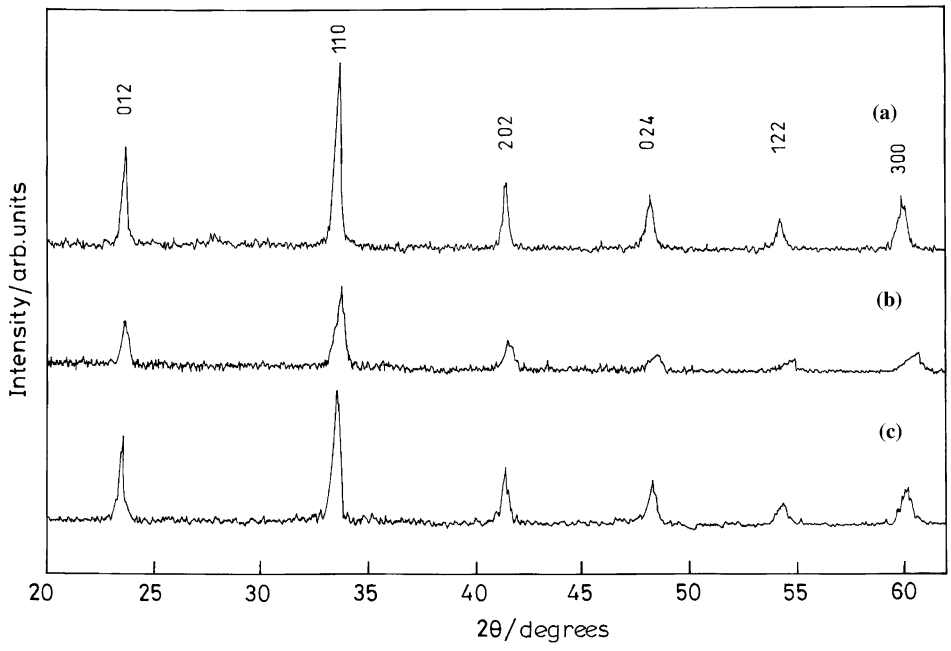

Fig. 3. Powder X-ray diffraction patterns of (a) $LaAlO_3$, (b) $NdAlO_3$ and (c) $PrAlO_3$ obtained after heat treatment of the precursors.

were compared with those reported for the corresponding perovskite oxide in the JCPDS Powder Diffraction Files and were indexed accordingly. Due to the poor crystallinity of the $LnMnO_3$ (Ln = Pr, Nd) oxides, these were indexed to a cubic cell. In all the cases, single-phase perovskite oxides could be obtained. The cell parameters and the PDF data with which the comparison was carried out are listed in Table 1. While all these studies have been made on electrosynthesized polycrystalline powders, we considered it important to demonstrate the synthesis of at least one of these as an adherent coating. The $LaAlO_3$ system was picked. In Figure 6 we show the XRD pattern of a $LaAlO_3$ coating obtained by thermal treatment of the corresponding

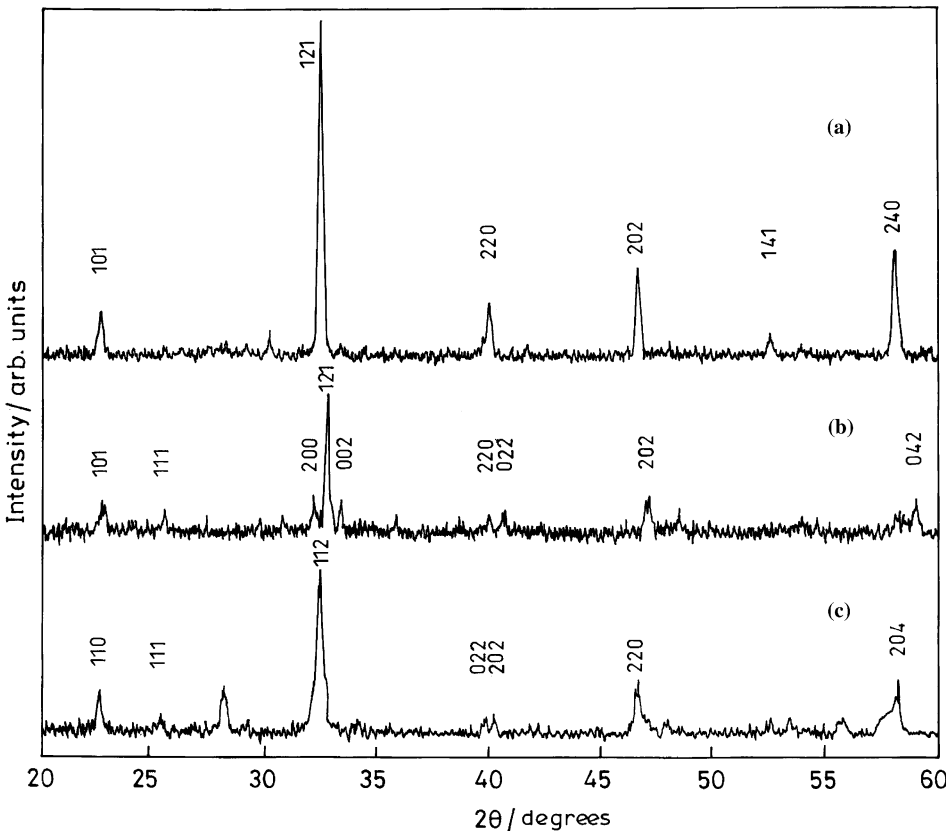

Fig. 4. Powder X-ray diffraction patterns of (a) $LaFeO_3$, (b) $NdFeO_3$ and (c) $PrFeO_3$ obtained after heat treatment of the precursors

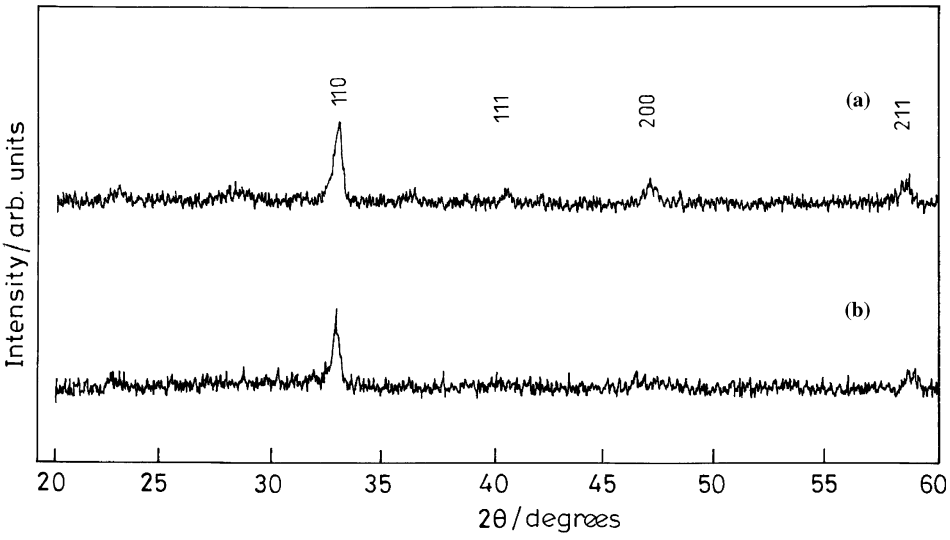

Fig. 5. Powder X-ray diffraction patterns of (a) $PrMnO_3$ and (b) $NdMnO_3$ obtained after heat treatment of the precursors.

hydroxide coating. It is clear that the oxide coat is that of $LaAlO_3$. In Figure 8 is shown a scanning electron micrograph of the $LaAlO_3$ coating, which clearly shows that the substrate is completely covered.

Electrosynthesis of perovskite oxides reported by Matsumoto and coworkers [14–18] are of those containing M^{3+} ions, which have been done by the anodic oxidation method. Anodic oxidation of a solution containing M^{2+} (M = Mn, Co, Ni) leads to the formation of higher valent oxides (MnO_2, Mn_2O_3 and Mn_3O_4 in the Mn system, NiOOH and CoOOH in the Ni and Co systems, respectively) in the precursor material. La^{3+} does not participate in any of the anodic reactions and its incorporation into the anodic oxide coating has to take place by adsorption. For successful incorporation of the La^{3+} ions, the bath has to be enriched in La^{3+} by a factor of 10^2–10^3 times the M^{2+} ion. Cathodic reduction, on the other hand, is a more elegant method as both Ln^{3+} and M^{2+} (as well as M^{3+}) coprecipitate as their respective hydroxides.

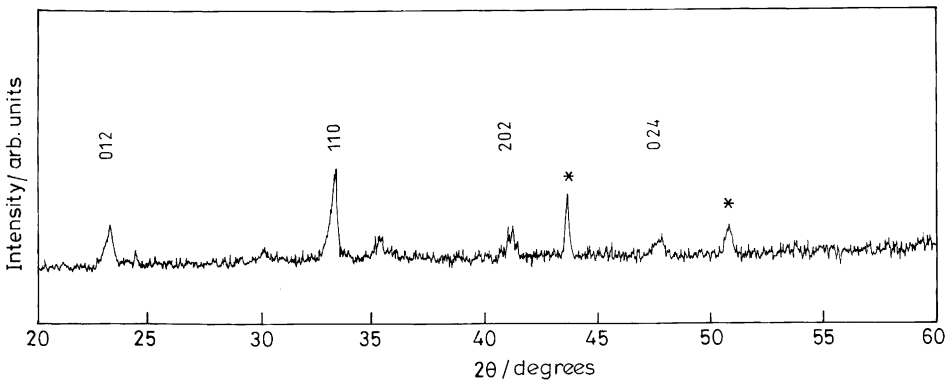

Fig. 6. Powder X-ray diffraction pattern of $LaAlO_3$ coating obtained on a stainless steel substrate. *Corresponds to substrate peak.

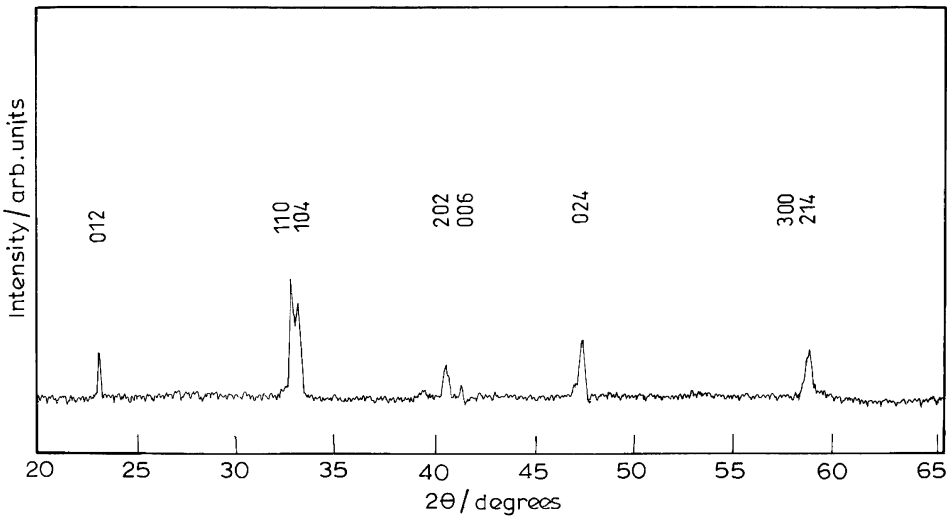

Fig. 7. Powder X-ray diffraction pattern of $LaCoO_3$.

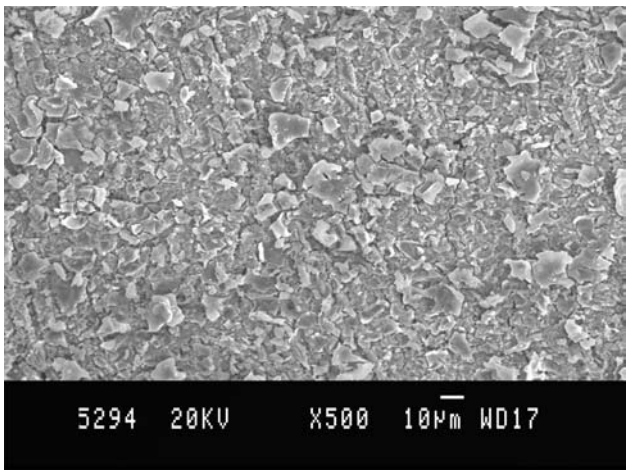

Fig. 8. Scanning electron micrograph of a coating of $LaAlO_3$ on a stainless steel substrate.

However, on account of the difference in their solubility products, the composition of the deposit varies from that of the bath. The bath composition was therefore empirically optimized to obtain a single-phase perovskite oxide on thermal treatment.

A solution of Fe^{3+} on electroreduction leads to the formation of a gel. In the presence of La^{3+}, on the other hand, Fe^{3+} coprecipitates as a pale brown X-ray amorphous coating. TG studies indicate that this precursor corresponds to the chemical formula $LnFe(OH)_6$. The precursor obtained from the Al containing solution could not be characterized, as the mass loss observed in TG does not correspond to any of the possible decomposition reactions. The observation of strong nitrate related vibrations in the precursor points to the possibility of the precursor being a hydroxy salt. This could not be verified in the absence of X-ray data.

In conclusion various perovskite oxides in both powder and coating form have been synthesized by cathodic reduction of mixed metal nitrate solutions by suitably choosing the deposition parameters such as bath composition, duration of synthesis and the temperature for heat treatment.

Acknowledgements

PVK thanks the University Grants Commission, Government of India, for financial support through the award of a Major Research Project. The authors thank the Solid State and Structural Chemistry Unit, Indian Institute of Science for powder X-ray diffraction facilities.

References

1. J.B. Goodenough, *Prog. Solid State Chem.* **5** (1971) 149.
2. J.B. Goodenough, J.M. Longo and L.B. Tabellen, *New Series III/4a* (Springer Verlag, Berlin, 1970).
3. C.N.R. Rao and K.J. Rao, *Phase Transitions in Solids* (McGraw Hill, NY, 1978).
4. M.S.D. Read, M.S. Islam, G.W. Watson, F. King and F.E. Hancock, *J. Mater. Chem* **10** (2000) 2298.
5. J. Töpfer and J.B. Goodenough, *J. Solid State Chem.* **130** (1997) 117.
6. A. Hammouche, E. Siebert and A. Hammoue, *Mat. Res. Bull.* **367** (1989) 24.
7. K.M. Sathyalakshimi, S.S. Manoharan, M.S. Hegde, V. Prasad and S.V. Subramaniam, *J. Appl. Phy.* **78** (1995) 6861.
8. S. Trasatti (Ed.), 'Electrodes of Conductive Metallic Oxides, Studies in Physical and Theoretical Chemistry' (Elsevier, Amsterdam, 1981), Vol. 11, Parts A & B.
9. H. Yugami, H. Naito, H. Arashi and M. Ishigame, *Solid State Ionics* **86** (1996) 1307.
10. B.Y. Liaw, R.E. Rocheleau and Q.-H. Gao, *Solid State Ionics* **92** (1996) 85.
11. M. Hartmanova, I. Thurzo, M. Jergel, J. Bartos, F. Kadlec, V. Zelezny, D. Tunega, F. Kundracik, S. Chromik and M. Brunel, *J. Mater. Sci.* **33** (1998) 969.
12. G.H.A. Therese and P.V. Kamath, *Chem. Mater* **12** (2000) 1195.
13. I. Zhitomirsky, *Am. Cerm. Soc. Bull.* (September 2000) 57.
14. T. Sasaki, Y. Matsumoto, J. Hombo and Y. Ogawa, *J. Solid State Chem.* **91** (1991) 61.
15. T. Sasaki, Y. Matsumoto, J. Hombo and M. Nagata, *J. Electroanal. Chem.* **371** (1994) 241.
16. Y. Matsumoto, H. Ohmura and T. Goto, *J. Electroanal. Chem.* **399** (1995) 91.
17. Y. Matsumoto, T. Sasaki and J. Hombo, *Inorg. Chem.* **31** (1992) 738.
18. Y. Matsumoto, T. Sasaki and J. Hombo, *Electrochim. Acta* **38** (1993) 1145.
19. G.H.A. Therese and P.V. Kamath, *Chem. Mater.* **10** (1998) 3364.
20. Z.P. Xu and H.C. Zeng, *J. Mater. Chem.* **8** (1998) 2499.
21. H. Bode, K. Dehmelt and J. Vitte, *Electrochim. Acta* **11** (1966) 1079.
22. J. Ismail, M.F. Ahmed and P.V. Kamath, *J. Power Sources* **36** (1991) 507.
23. D.A. Corrigan and R.M. Bendert, *J. Electrochem. Soc.* **136** (1989) 723.
24. Y. Matsumoto, T. Morikawa, H. Adachi and J. Hombo, *Mat. Res. Bull.* **27** (1992) 1319.
25. J.A. Switzer, *Am. Ceram. Soc. Bull.* **66** (1987) 1521.
26. G.H.A. Therese and P.V. Kamath, *Chem. Mater.* **11** (1999) 3561.
27. L. Indira and P.V. Kamath, *J. Mater. Chem.* **4** (1994) 1487.